Hindawi
Geofluids
Volume 2021, Article ID 5510566, 9 pages
https://doi.org/10.1155/2021/5510566

Research Article

A Case Study on the Gas Drainage Optimization Based on the Effective Borehole Spacing in Sima Coal Mine

Ming Ji,[1] **Zhong-guang Sun**,[2,3,4] **and Wei Sun**[3]

[1]*Key Laboratory of Deep Coal Resource Mining, Ministry of Education of China and China University of Mining & Technology, Xuzhou 221116, China*
[2]*State Key Laboratory of The Gas Disaster Detecting, Preventing and Emergency Controlling, Chongqing 400037, China*
[3]*China Coal Technology and Engineering Group Chongqing Research Institute, Chongqing 400039, China*
[4]*State Key Laboratory for the Coal Mine Disaster Dynamics and Controls, Chongqing University, Chongqing 400044, China*

Correspondence should be addressed to Ming Ji; jiming@cumt.edu.cn

Received 26 February 2021; Revised 15 June 2021; Accepted 14 August 2021; Published 8 September 2021

Academic Editor: Yi Xue

Based on the dynamic expressions of permeability and porosity of the coal seam derived in the paper, a multiphysical field coupling numerical model of gas migration under the interaction of stress field and seepage field was established. The gas drainage project #3 Coal Seam operated by Sima Coal Industry Co., Ltd., was selected as the study object. Taking different drainage time periods in various positions of drainage holes into consideration, combined with the advance situation of the 1207 working face in the Sima Coal Mine, a mixed layout gas drainage scheme featured with the effective borehole spacing was obtained through the COMSOL multiphysics simulation. In addition, a series of field industrial tests were performed to validate the research result, revealing that comprehensively considering the extraction time of coal and optimizing the layout of extraction boreholes can effectively improve the engineering economic benefits.

1. Introduction

Coal seam gas drainage is one of the important measures to control mine gas [1, 2] However, a majority of researches take the effective drainage radius as the basis of drainage hole layout, overlooking the influences of the superimposed drainage and fracture expansion without taking the influence of different drainage times of drainage holes in different positions of the coal seam into account. Additionally, most researches adopt a single borehole layout, which often causes some common issues such as a waste of resource, uneven gas drainage, and failure of meeting relevant standards. Many existing studies fail to consider the establishment of a multiphysical field coupling model of gas migration under the interaction of the stress field and seepage field and overlook the dynamic nature of the permeability and porosity of the coal seam. All the aforementioned which are lacking in previous studies have made it necessary to conduct an in-depth optimization research on coal seam gas drainage.

In this paper, the gas drainage optimization of #3 Coal Seam in Sima Coal Industry Co., Ltd., of Lu'an Group was studied. Based on the changes of coal seam stress, gas pressure, and gas adsorption and desorption which tend to exert an important impact on the coal seam permeability and porosity, the dynamic expressions of coal seam permeability and porosity were deduced which was used to build the numerical model of a multiphysical field coupling for migration under the interaction of stress field and seepage field. Additionally, taking different drainage time periods in various positions of drainage holes into consideration, combined with the advance situation of the 1207 working face in the Sima Coal Mine, a mixed layout gas drainage scheme featured with the effective borehole spacing was obtained by the COMSOL multiphysics simulation. In addition, a series of field

industrial tests were performed for the purpose of validating the research.

2. Gas Solid Coupling Analysis of Coal Seam Gas Migration

2.1. The Migration Law of Coal Seam Gas. Two types of gas flow in coal seams have been identified including the diffusion flow and the laminar flow targeting different types of coal seams [3–5]. Generally speaking, in the coal seam with a microporous structure or low permeability, the diffusion flow plays a critical role while in the coal seam with microporous structure or high permeability, the laminar flow dominates [6–8]. In this study, the gas flow in the process of drainage is treated as laminar flow, following Darcy's law.

A number of factors can affect the migration of coal seam gas, such as geological conditions of storage, occurrence of coal seam, mechanical properties of coal and rock, permeability and porosity of coal seam, gas adsorption capacity of coal seam, and gas pressure. Among those factors, gas pressure, gas adsorption capacity of coal seam, porosity, and permeability of coal seam are considered as the primary ones. Gas pressure is the driving force of gas migration while the gas adsorption capacity of coal seam decides the capacity of the coal seam to store gas. Meanwhile, the porosity and permeability are the indicators of smooth gas migration in the coal seam [9–11].

The gas pressure of the #3 Coal Seam in Sima mine was measured at 0.31 MPa which was used as the basic gas pressure of this study, despite that the gas pressure measured stayed below the critical value of 0.74 MPa. The gas adsorption constants a and b of the #3 Coal Seam were identified at about 17.52 $m^{3/}t$ and 0.75 MPa^{-1}, separately, which were considered low, indicating that the gas adsorption capacity of the #3 Coal Seam was weak. During the field drainage, several measures can be adopted to facilitate the drainage and extraction including the selection of the appropriate negative pressure of the drainage hole, the optimization of the layout of the hole, the promotion of the desorption of gas, and the increase of the gas diffusion and migration speed.

2.2. The Derivation of Dynamic Expressions of Porosity and Permeability of Coal Seam. During the gas extraction, the gas tends to be desorbed and migrated, exposing the coal skeleton to stress changes, resulting in small deformation, and the porosity and permeability change accordingly. According to the existing research and the field conditions of Sima mine and the 2D model in the numerical simulation calculation, the plane strain ε_s is introduced, leading to a modified dynamic expression of coal seam porosity [12–14].

$$\varphi = 1 - \frac{1-\varphi_0}{1+\varepsilon_s}\left(1 - \frac{\Delta p}{k_s}\right), \tag{1}$$

where φ_0 is the initial porosity of coal, ε_v is the volume strain, ΔP is the variation of gas pressure, $\Delta p = P - P_0$, P is the real time gas pressure, P_0 is the initial gas pressure, and k_s is the skeleton modulus of the coal and rock mass.

According to the Kozeny-Carman formula, combined with the previous dynamic expression of porosity, the modified dynamic expression of permeability can be obtained as follows:

$$k_e = \frac{k_0}{1+\varepsilon_s}\left[1 + \frac{\varepsilon_s + (\Delta p/k_s)(1-\varphi_0)}{\varphi_0}\right]^3, \tag{2}$$

where k_0 is the initial permeability of coal and ε_s is the plane strain.

2.3. The Multiphysical Field Coupling Model of Coal Seam Gas Migration. This study focuses on the deformation of the coal seam due to the forces imposed and the gas flow [15–18]. Therefore, the following assumptions have been made:

(1) The flow field formed by the gas drainage hole under a certain negative pressure is the radial flow field

(2) The adsorption content of the gas is described by the Langmuir equation

(3) Gas flow is described by Darcy's law

(4) The seepage process of the gas is regarded as an ideal isothermal process

(5) The coal seam is isotropic with only a small linear elastic deformation

(6) The influence of water in the coal seam on gas drainage is overlooked

Taking the assumptions listed above into consideration, the seepage movement of coal seam gas as the ideal gas should follow the control equations of gas flow listed as follows [13, 14, 19–25].

2.3.1. Law of Conservation of Mass. Gas in the coal seam often takes two forms including the free state and the adsorption state. Despite the statuses, the source and total amount of gas in the coal seam remain unchanged. In other words, the gas migration should first follow the law of conservation of mass:

$$\frac{\partial m}{\partial t} + \nabla \bullet \left(\rho_g q_g\right) = Q_p, \tag{3}$$

where m is the gas content (kg/m^3), ρ_g is the gas density (kg/m^3), q_g is the Darcy seepage velocity of gas (m/s), Q_p is the source or sink items (kg/(m^3·s)), and t is the time variable (s).

2.3.2. The State Equation of Gas. The gas in seepage movement is regarded as an ideal gas, which satisfies the equation of state of ideal gas:

$$\rho_g = \frac{M_g P}{RT}, \tag{4}$$

where M_g is the molecular weight of gas (kg/kmol), P is the gas pressure (Pa), R is the ideal gas constant (kJ/(kmol·K)), and T is the absolute temperature (K_o).

2.3.3. Langmuir Equation. The coal seam is a porous medium with many pores and fissures, in which gas coexists in the adsorption state and the free state. The Langmuir equation describing the gas content defines the relationship between gas adsorption and desorption with gas pressure:

$$m = \frac{M_g}{RT}\left(\frac{\varphi}{P_0} + \frac{ab\rho_s}{1+bP}\right)P^2, \tag{5}$$

where φ is the porosity, P_0 is the atmospheric pressure (Pa), a is the Langmuir constant (m^3/kg), b is the Langmuir constant (Pa^{-1}), and ρ_s is the coal seam density (kg/m^3).

2.3.4. Darcy's Law. When a pressure gradient is identified in the distribution of gas pressure in the coal seam, the gas migration will occur, which is often a linear seepage flow and follows Darcy's law:

$$q_g = -\frac{k_e}{\mu_g}\left(\nabla p + \rho_g g \nabla z\right)^2, \tag{6}$$

where q_g is the Darcy flow velocity (m/s), k_e is the permeability of the coal seam (m^2), μ_g is the gas dynamic viscosity (Pa·s), and g is the acceleration of gravity ($m \cdot s^{-2}$).

The process of gas extraction is featured with two physical phenomena including the seepage movement of gas as fluid and the microdeformation of coal. The stress and deformation of the coal body cause changes to the pore characteristics and then affect the gas seepage movement. Consequently, the gas seepage tends to change the gas pressure within the coal body, resulting in different effective stresses. The interaction of two phenomena acts like a chain reaction featured with mutual constraint and influence.

The dynamic expression of coal seam porosity is substituted into equation (5), then

$$m = \frac{M_g}{RT}\left[\frac{1}{P_0} - \frac{1-\varphi_0}{P_0(1+\varepsilon_s)}\left(1-\frac{\Delta P}{k_s}\right) + \frac{ab\rho_s}{1+bP}\right]P^2. \tag{7}$$

The dynamic expression of coal seam permeability is substituted into equation (6), then

$$q_g = -\frac{k_0\left(\nabla p + \rho_g g\nabla z\right)^2}{\mu_g(1+\varepsilon_s)}\left[1+\frac{\varepsilon_s + (\Delta p/k_s)(1-\varphi_0)}{\varphi_0}\right]^3. \tag{8}$$

By substituting formula (4) and derived formulas (7) and (8) into formula (3), the following results are obtained:

$$\frac{\partial\left\{(M_g/RT)[1/P_0 - ((1-\varphi_0)/P_0(1+\varepsilon_s))(1-\Delta P/k_s) + ab\rho_s/(1+bP)]P^2\right\}}{\partial t} - \nabla \cdot \left\{\frac{M_g P k_0\left(\nabla p + \rho_g g\nabla z\right)^2}{RT\mu_g(1+\varepsilon_s)}\left[1+\frac{\varepsilon_s + (\Delta p/k_s)(1-\varphi_0)}{\varphi_0}\right]^3\right\} = Q_p. \tag{9}$$

Formula (9) is the gas-solid coupling model finally derived in this paper. The model is embedded into the COMSOL multiphysics software for gas drainage optimization.

Table 1: Model parameter.

Items	Symbol	Value
Gas density (kg/m^3)	rhog	0.716
Gas dynamic viscosity (Pa·s)	vl	1.08*e*-5
Equivalent compressibility of matrix (1/Pa)	χ_p	2.18*e*-3
Fluid compressibility (1/Pa)	chif	1.3942*e*-5
Coal density (kg/m^3)	rhoc	1470
Initial porosity of coal	φ_0	0.0318
Poisson's ratio of coal	mu	0.33
Initial permeability of coal (m^2)	k_0	0.907*e*-15
Young's modulus of coal (MPa)	E	3000
Initial pressure of coal gas (MPa)	P_0	0.31
Standard atmospheric pressure (Pa)	P_a	1.01*e*5
Biot-Willis coefficient	α_B	0.801

3. The Introduction of the Calculation Model

3.1. The Calculation Model Parameter Setting. Before establishing the numerical model, the determination of the relevant parameters involved is vital. Based on relevant literature and geomechanics tests, after testing and adjusting the coefficient of the COMSOL multiphysics 5.0 built-in module, the main parameters used in the model were obtained, as shown in Table 1.

3.2. The Model Establishment. The original gas pressure of the #3 Coal Seam in the Sima mine was 0.31 MPa. Due to the large error of gas concentration measurement, the original gas pressure reduced by 30% was selected as the standard for the simulation, leading to setting the gas drainage standard pressure at 0.22 MPa.

In order to provide direct guidance to the field construction, the effective borehole spacing was introduced in the simulation. The gas pressure of the whole seam can be reduced to the maximum borehole spacing value within the standard pressure value after drainage for a certain period of time. In other words, through the numerical simulation, the most reasonable drilling spacing value can be determined, which not only meets the need of reducing gas pressure but also reduces the difficulty and cost of on-site construction.

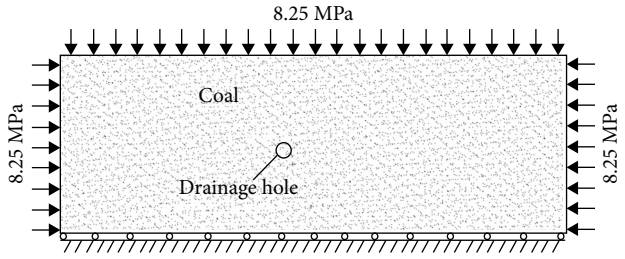

Figure 1: The calculation model.

The method similar to the "bucket theory" was used to calculate the effective drilling spacing, aiming to find out the area with the least superimposed effect of borehole pumping in the simulation calculation model and ensure that the pressure within the area drops right below the standard value.

The porous elastic module and Darcy's law module [13, 14, 26] in COMSOL were used in this simulation, and the required variables and parameters were inputted to the software. According to the actual drilling gas drainage process, an idealized two-dimensional calculation model with length × height of 16 m × 6.6 m was established as shown in Figure 1. The drainage boreholes were arranged in the middle of the model with the bottom as a fixed constraint. Meanwhile, the upper, left, and right boundaries have a boundary load of 8.25 MPa as the actual confining pressure condition. All sides of the model were airtight with an initial gas pressure of 0.31 MPa in the model.

As demonstrated in Figure 1, a drill hole was arranged in the 2D calculation module. Following the single variable method, the effective extraction radius corresponds to various diameters of extraction drill holes (95 mm, 113 mm, and 133 mm), extraction pressures (20 kPa, 25 kPa, 30 kPa, 35 kPa, 40 kPa, and 45 kPa), and extraction durations (90 d, 180 d, and 360 d). The detailed calculations are presented in Table 2.

According to Table 2, as the extraction duration, pressure, and diameter of the extraction drill hole increased, the effective radius of the single drainage hole increased, demonstrating a positive correlation.

Currently, the commonly adopted extraction drill holes are sized at113 mm in diameter and 133 mm in diameter, with the extraction pressure between 25 kPa and 40 kPa. The extraction often consumes substantial time, more than 1 year and even 2 to 3 years. Due to the relatively thicker coal seal in the Sima mine, multiple extraction holes in multiple layers were adopted. The extraction holes are often arranged in three ways including the three-flower style, four-flower style, and five-flower style, as demonstrated in Figure 2.

A few simulations with various conditions were performed including the extraction drill holes of 113 mm and 133 mm in diameter under the extraction pressure of 25 kPa, 30 kPa, 35 kPa, and 40 kPa. The extraction duration was set at 360 d. The calculation of the effective extraction radius is demonstrated in Figure 3 below.

Table 2: The simulation results of single-bore model.

Single bore		Effective radius of drainage (m)		
Hole diameter	Negative pressure	90 d	180 d	360 d
95 mm	20 kPa	0.45	0.57	0.72
95 mm	25 kPa	0.46	0.57	0.73
95 mm	30 kPa	0.46	0.58	0.74
95 mm	35 kPa	0.47	0.59	0.75
95 mm	40 kPa	0.47	0.60	0.76
95 mm	45 kPa	0.48	0.61	0.77
113 mm	20 kPa	0.48	0.60	0.76
113 mm	25 kPa	0.48	0.61	0.77
113 mm	30 kPa	0.49	0.62	0.78
113 mm	35 kPa	0.49	0.62	0.79
113 mm	40 kPa	0.50	0.63	0.80
113 mm	45 kPa	0.51	0.64	0.81
133 mm	20 kPa	0.50	0.63	0.80
133 mm	25 kPa	0.51	0.64	0.81
133 mm	30 kPa	0.51	0.65	0.82
133 mm	35 kPa	0.52	0.66	0.83
133 mm	40 kPa	0.53	0.67	0.84
133 mm	45 kPa	0.53	0.67	0.85

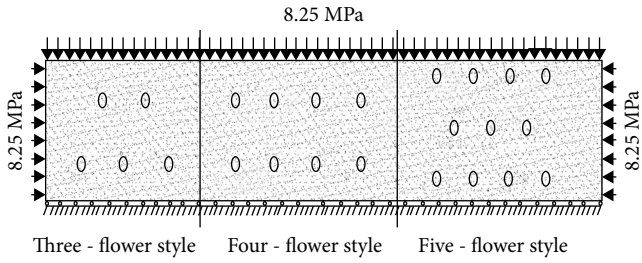

Figure 2: Three arrangements of drainage holes.

According to Figure 3, the drainage hole of 133 m in diameter demonstrated better extraction. The negative pressure of the extraction hole was 35kpa in the coal mining practice. The five-flower layout of the extraction holes was superior than the three-flower layout while the three-flower layout is superior the four-flower layout.

4. The Simulation and Analysis of the 1207 Working Face of Sima Coal

4.1. The Simulation Process Analysis. The strike length of the 1207 working face in the #3 Coal Seam of the Sima mine is 220 m with an inclined length of 1092 m. During the production, in order to ensure the safety of production, gas extraction was carried out. However, this kind of pumping scheme is single without considering the specific circumstances.

As mentioned previously, the drainage time greatly affects the gas drainage. Different drainage time periods should adopt different drainage hole layout schemes, such

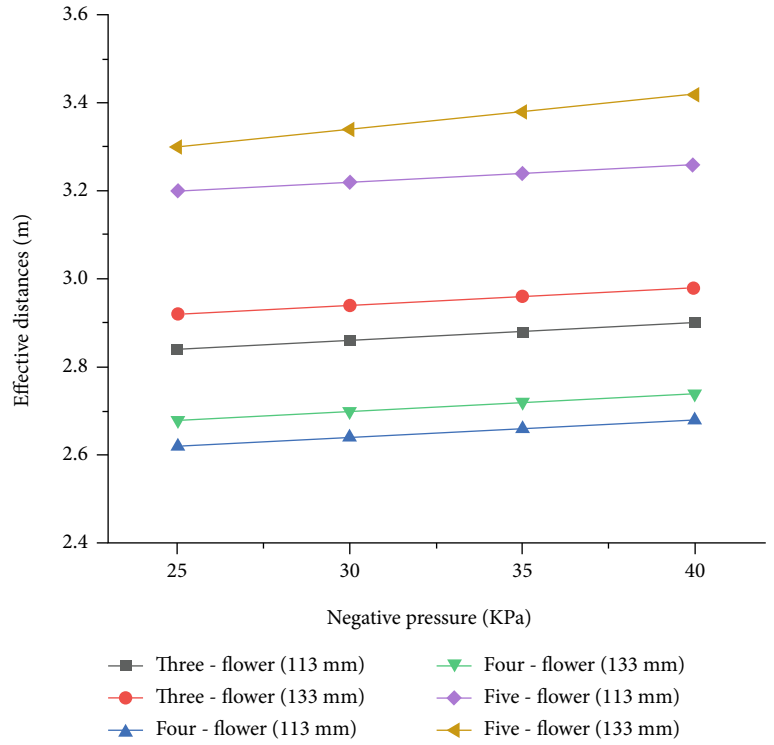

Figure 3: The effective distances between bores under different suction pressures.

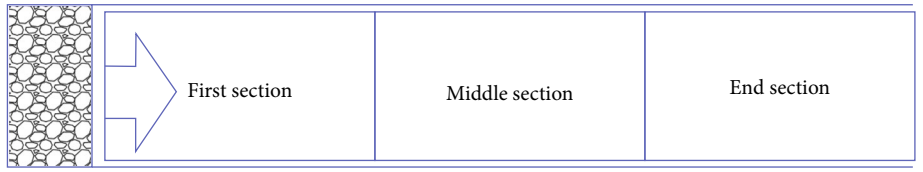

Figure 4: The sections divided in the roadway for extraction.

as different borehole spacings or patterns. As the no. 1207 working face advanced, different extraction durations were identified in different positions of extraction boreholes in the mining roadway. Under such circumstance, different sections should be divided based on the different extraction durations, allowing individual extraction design corresponding to different field conditions.

According to the comprehensive analysis of the driving speed, working face layout time, and mining speed of the mining roadway in the no. 1207 working face, and taking the drainage effectiveness into consideration, the coal seam gas drainage in the no. 1207 working face can be divided into three sections in simulation, as shown in Figure 4. The average extraction time of the three sections is 110D, 210D, and 310D, respectively.

The average extraction time, negative pressure, and hole diameter of the three sections were identified, and the gas extraction optimization of the three sections was also studied in detail. The calculation model of the optimization of the extraction changes from the single-row hole layout to the five-row pattern hole layout until the optimal result was obtained. Under the extraction of the experimental scheme, the goal of the whole layer of the #3 coal extraction up to 0.22 MPa was achieved.

4.2. The Analysis of Simulation Results

4.2.1. The Analysis of the First and Middle Sections. The extraction time of the first section and the middle section was set at 110 days and 210 days, respectively. According to the simulation calculation, the coal seam gas pressure can be reduced to the standard value within a fixed time only when the five-flower layout was adopted. Due to the different extraction durations, the effective drilling spaces of the two sections varied. The gas pressure cloud diagram in the simulation process is shown in Figures 5(a) and 5(b).

According to Figure 5, with more gas extraction, the pressure of the gas in the coal seam experienced constant changes. The gas pressure closer to the drainage hole dropped most. A further distance from the drainage hole leads to less decrease in the gas pressure until the threshold distance was reached where the gas pressure stayed at the initial value, indicating that the coal outside the impact boundary was not subject to the impacts of the extraction.

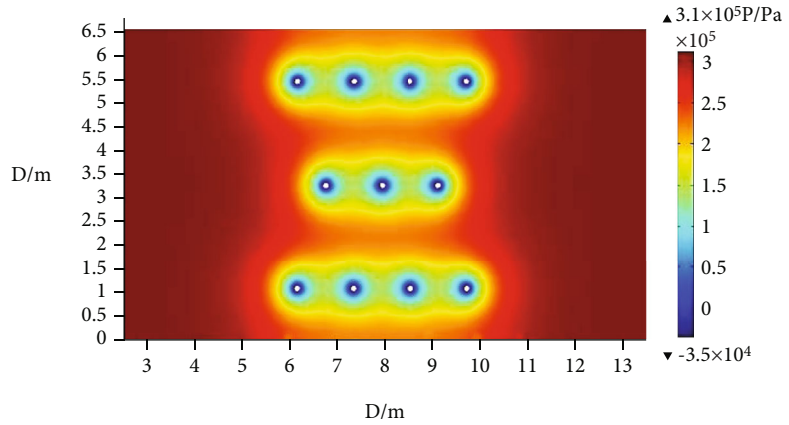

(a) The first section

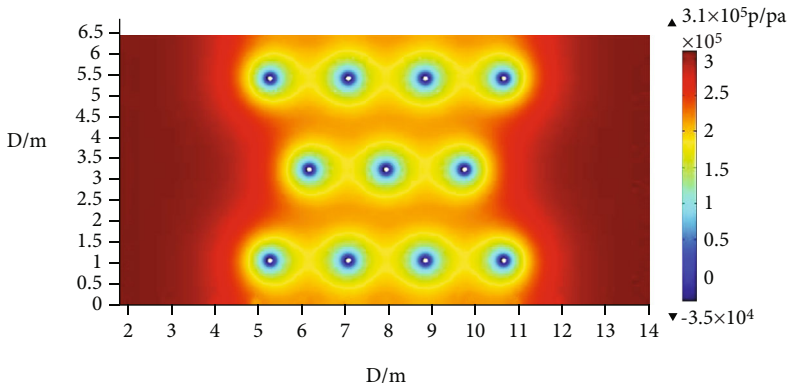

(b) The middle section

Figure 5: The gas pressure cloud diagram from simulation.

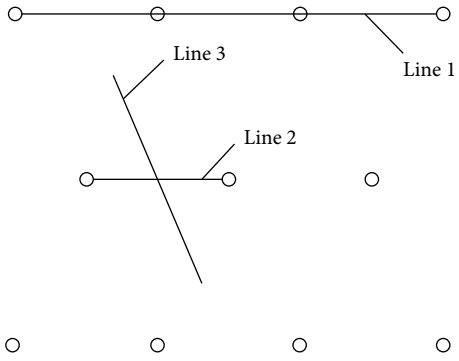

Figure 6: The structure line of the value line graph.

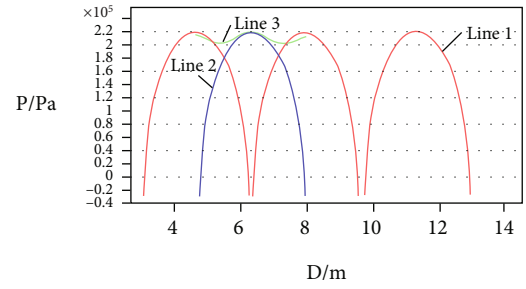

Figure 7: The value line graph.

In order to describe the gas pressure distribution in the five-flower arrangement, the structure line of the value line graph shown in Figure 6 was inserted into the simulated gas pressure cloud graph, which can vividly illustrate the distribution of the gas pressure value in the area wrapped by the five-flower hole. The value line graph is shown in Figure 7.

According to Figure 5, the maximum gas pressure in the wrapping area of the five-flower hole is 0.22 MPa, and the gas pressure in other places is lower than the set value. At this time, the distance between two adjacent drainage holes at the same level is concluded as the effective drilling spacing.

Table 3: Effective borehole spacing values in different sections.

Roadway segmentation	Extraction time	Horizontal effective drilling spacing value	Longitudinal row spacing
First segmentation	110 d	1.15 m	2.20 m
Middle segmentation	210 d	2.45 m	2.25 m

According to the simulation results, the effective drilling spacing values of the two sections in the five-flower arrangement are obtained, as shown in Table 3.

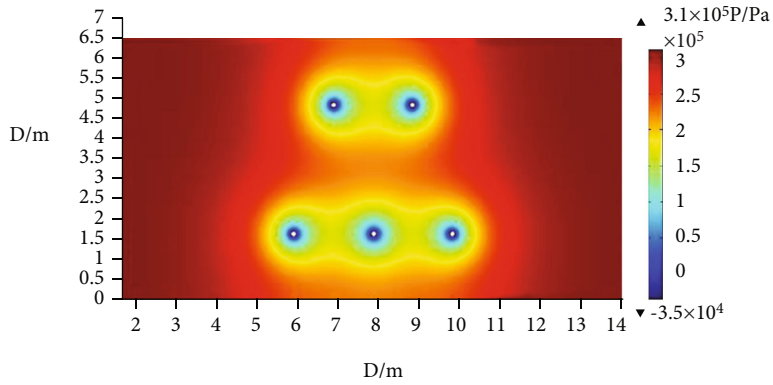

Figure 8: The gas pressure cloud diagram.

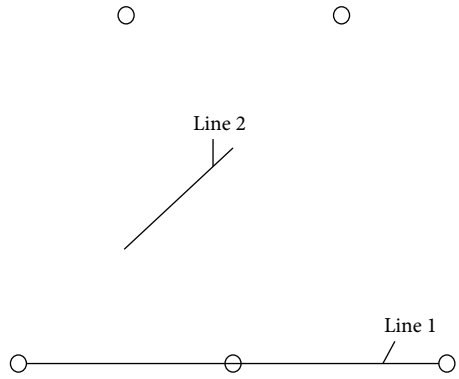

Figure 9: The structure line of the value line graph.

4.2.2. The Analysis of the Results of the End Sections. The extraction time of the end section was set at 310 days. The simulation suggests that the coal seam gas pressure can be reduced to the standard value within a fixed time when the three-flower arrangement was adopted. The gas pressure cloud diagram in the simulation process is shown in Figure 8.

Similarly, from Figure 8, being closer to the drainage hole leads to higher pressure drops. The gas pressure reaches the peak value of 0.22 MPa at the triangle center of gravity. In order to better describe the distribution of gas pressure in the three-flower hole, the construction line of the value-taking line diagram shown in Figure 9 was inserted into the simulated gas pressure cloud diagram, which can vividly illustrate the distribution of the gas pressure value in the area wrapped by the three-flower hole, and the value-taking line diagram is shown in Figure 10.

According to Figure 10, the maximum gas pressure in the wrapping area of the three-flower hole is 0.22 MPa, and the gas pressure in other places is lower than the set value. At this time, the distance between two adjacent extraction holes at the same level is the effective drilling spacing.

The simulation has suggested that the horizontal effective spacing between boreholes is 2.00 m with the vertical row spacing of 2.00 m when the three-flower pattern layout is adopted in the end section.

4.3. A Proposal of a Mixed Layout Scheme. According to the previous calculation results, a mixed layout scheme was developed specifically for the gas drainage in the no. 1207 working face of the Sima mine. The details are presented as follows.

The first section: a five-flower pattern layout was adopted with the horizontal drilling spacing of 1.15 m. The upper row of drilling is 5.50 m away from the floor longitudinally with the middle row of drilling 3.30 m away from the floor, and the bottom row of drilling1.10 m away from the floor.

The middle section: a five-flower pattern layout is adopted with the horizontal drilling spacing as 2.45 m. The upper row of drilling was 5.55 m away from the floor longitudinally with the middle row of drilling 3.30 m away from the floor, and the bottom row of drilling1.05 m away from the floor.

The end section: a three-flower pattern arrangement was adopted with the horizontal drilling spacing as 2.00 m. The upper row of drilling was 4.92 m away from the floor longitudinally with the bottom row of drilling 1.68 m away from the floor.

5. The Industrial Test

5.1. The Detailed Test Plan. In this industrial practice, the air-return roadway of the no. 1207 working face was selected. Without affecting the original production and extraction, the extraction practice test was carried out at 450 m~485 m in the middle section and 750 m~785 m in the end section of the air-return roadway. According to the previous calculation results, the specific scheme is proposed as follows:

(1) At 450 m~485 m in the middle section of the air-return roadway

The five-flower hole layout was adopted along with a negative pressure of 35 kPa, a diameter of 133 mm, an average length of 161 m, and a horizontal drilling spacing of 2.45 m. Longitudinally, the upper row of holes was 5.55 m away from the floor, with the middle row of holes 3.30 m away from the floor, and the bottom row of holes 1.05 m away from the floor.

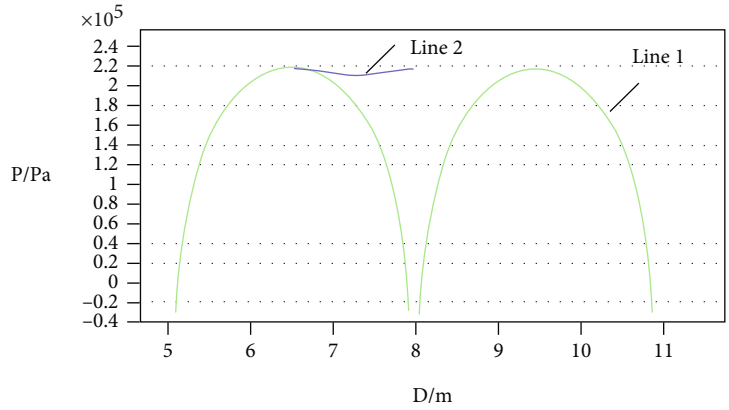

Figure 10: The value line graph.

(2) At 750 m~785 m in the end section of the air-return roadway

The three-flower hole layout was adopted with a negative pressure of 35 kPa, a diameter of 133 mm, an average length of 161 m, and a horizontal drilling spacing of 2.00 m. Longitudinally, the distance between the upper row and the floor was 4.92 m, with the distance between the bottom row and the floor at 1.68 m.

5.2. The Analysis of the Field Test. The industrial test scheme for gas drainage revealed that the drainage boreholes cover the coal seam effectively and evenly. The residual gas content in the middle and end sections of the air roadway was reduced by 31.24% and 32.16%, respectively, with the analytic gas content reduced by 46.86% and 49.81%, respectively, and the coal seam gas pressure reduced by 45.03% and 48.33%, respectively.

6. Conclusion

As the extraction duration, the negative pressure of the extraction, and the extraction drill hole diameter increase, the effective extraction radius of the single drainage hole increases, demonstrating a positive correlation.

Based on the simulation, a proposal including an effective spacing among extraction holes was developed. In the proposal, the extraction holes are arranged based on the effective drainage hole distances, taking various extraction durations corresponding to different locations in the roadway into consideration.

According to the gas pressure cloud diagram, a greater pressure drop is identified closer to the extraction hole. The gas pressure stays stable after reaching the threshold distance.

The gas pressure decreases with the increase of extraction time and finally grows stable. Some superposition effects have been identified between two drainage holes with a more intensive gas pressure drop in the superposition area.

Data Availability

The data used to support the findings of this study are available from the corresponding author upon request.

Conflicts of Interest

The authors declare that there are no conflicts of interest regarding the publication of this paper.

Acknowledgments

This paper was supported by the Priority Academic Program Development of Jiangsu Higher Education Institutions and the Natural Science Foundation of Chongqing, China (Grant No. cstc2019jcyj-msxmX0633 and No. cstc2020jcyj-msxmX0972), and the Science and Technology Planning Project of Jiulongpo District, China (Grant No. 2020-02-005-Y).

References

[1] Z. Yan, Y. Wang, J. Fan, Y. Huang, and Y. He, "Study on key parameters of directional long borehole layout in high-gas working face," *Shock and Vibration*, vol. 2021, Article ID 5579967, 14 pages, 2021.

[2] X. Guo, S. Xue, Y. Li, C. Zheng, and L. Xie, "Research on optimization of key areas of drainage borehole sealing in ultrathick coal seam," *Shock and Vibration*, vol. 2021, Article ID 5536196, 8 pages, 2021.

[3] J. Fan, *Research and Application of Gas Drainage Technology in Working Face of High Gas Coal Seam*, China Coal Research Institute, 2016.

[4] R. Pan, *Permeability evolution characteristics of loaded coal and its application in pressure relief gas drainage*, China University of mining and technology, 2014.

[5] J. Z. Zhou, C. F. Wei, W. T. Li, and H. L. Chen, "Analysis of saolid elastoplastic mechanics based on mathematical module of COMSOL Multiphysics," *Engineering Journal of Wuhan University*, vol. 48, no. 2, pp. 195–201, 2015.

[6] L. Si, H. Zhang, J. Wei, B. Li, and H. Han, "Modeling and experiment for effective diffusion coefficient of gas in water-saturated coal," *Fuel*, vol. 284, no. 15, article 118887, 2021.

[7] L. Si, J. Wei, Y. Xi et al., "The influence of long-time water intrusion on the mineral and pore structure of coal," *Fuel*, vol. 290, article 119848, 2021.

[8] F. Wang, J. He, Y. Liang, Y. Luo, Z. Liao, and L. Li, "Study on the permeability characteristics of coal containing coalbed

methane under different loading paths," *Energy Science and Engineering*, vol. 6, no. 5, pp. 475–483, 2018.

[9] B. Li, S. Xue, and C. Zheng, "Enhancing gas pre-drainage system performance based on fault tree failure analysis for environmental safety," *Fresenius Environmental Bulletin*, vol. 30, no. 2A, pp. 2137–2146, 2021.

[10] Z. Cheng, H. Pan, and Q. Zou, "Gas flow characteristics and optimization of gas drainage borehole layout in protective coal seam mining: a case study from the Shaqu coal mine, Shanxi province, China," *Natural Resources Research*, vol. 30, no. 2, pp. 1481–1493, 2021.

[11] C. Zhang, J. Xu, E. Wang, and S. Peng, "Experimental study on the gas flow characteristics and pressure relief gas drainage effect under different unloading stress paths," *Geofluids*, vol. 2020, Article ID 8837962, 10 pages, 2020.

[12] T. Li, B. Wu, and B. Lei, "Study on the optimization of a gas drainage borehole drainage horizon based on the evolution characteristics of mining fracture," *Energies*, vol. 12, no. 23, article 4499, 2019.

[13] B. LI, J. Wei, and L. Peng, "Numerical simulation on gas drainage of boreholes in coal seam based on gas-solid coupling model," *Computer Modelling & New Technologies*, vol. 18, no. 12A, pp. 418–424, 2014.

[14] J. Wei, B. Li, K. Wang, and D. Sun, "3D numerical simulation of boreholes for gas drainage based on the pore-fracture dual media," *International Journal of Mining Science and Technology*, vol. 26, no. 4, pp. 739–744, 2016.

[15] S. Li, "Solid-gas coupling model and numerical simulation of coal containing gas based on COMSOL multiphysic," *Advanced materials research*, vol. 616-618, pp. 515–520, 2013.

[16] X. Yang and X. Zhao, "Study on influence of complex stress on fracture damage of coal and rock mass in pressure relief borehole," *Science and technology in China*, vol. 9, no. 2, pp. 138-139, 2015.

[17] L. Han, "Numerical simulation of gas drainage based on fluid-solid-heat coupling model," *Journal of Liaoning Technical University (Natural Science Edition)*, vol. 32, no. 12, pp. 1605–1608, 2013.

[18] C. Li, *Study on the Relationship between Drilling Parameters and Gas Drainage Effect in the Coal Seam*, Henan Polytechnic University, 2014.

[19] C. Liu, G. Yin, M. Li et al., "Shale permeability model considering bedding effect under true triaxial stress conditions," *Journal of Natural Gas Science and Engineering*, vol. 68, article 102908, 2019.

[20] C. Liu, G. Yin, M. Li, D. Shang, B. Deng, and Z. Song, "Deformation and permeability evolution of coals considering the effect of beddings," *International Journal of Rock Mechanics and Mining Sciences*, vol. 117, pp. 49–62, 2019.

[21] Z. Sun, L. Li, F. Wang, and G. Zhou, "Desorption characterization of soft and hard coal and its influence on outburst prediction index," *Energy Sources, Part A: Recovery, Utilization, and Environmental Effects*, vol. 42, no. 22, pp. 2807–2821, 2020.

[22] Y. Xue, J. Liu, P. G. Ranjith, X. Liang, and S. Wang, "Investigation of the influence of gas fracturing on fracturing characteristics of coal mass and gas extraction efficiency based on a multi-physical field model," *Journal of Petroleum Science and Engineering*, vol. 206, article 109018, 2021.

[23] S. Hu, G. Tao, and L. Xiaohong, "Analysis and numerical simulation of fluid-structure coupling of gas drainage from boreholes," *Journal of Chongqing University*, vol. 34, no. 11, pp. 105–110, 2011.

[24] S. Wei, K. Ma, and B. Li, "Research on coal and gas outburst based on COMSOL multiphysics," *Coal*, vol. 19, no. 5, pp. 14–16, 2010.

[25] G.-Z. YIN, L. I. Ming-Hui, L. I. Sheng-Zhou, L. I. Wen-Pu, J.-W. YAO, and Q.-G. ZHANG, "3d numerical simulation of gas drainage from boreholes based on solid gas coupling model of coal containing gas," *Journal of China Coal Society*, vol. 38, no. 4, pp. 535–541, 2003.

[26] H. P. Xie, H. W. Zhou, D. J. Xue, and F. Gao, "Theory, technology and engineering of simultaneous exploitation of coal and gas in China," *Journal of China Coal Society*, vol. 39, no. 8, pp. 1391–1397, 2014.